

PPAR α Regulates Mobilization and Homing of Endothelial Progenitor Cells Through the HIF-1 α /SDF-1 Pathway

Zhongxiao Wang,^{1,2} Elizabeth Moran,² Lexi Ding,^{2,3} Rui Cheng,² Xun Xu,¹ and Jian-xing Ma²

¹Department of Ophthalmology, Shanghai First People's Hospital Affiliated with Shanghai Jiaotong University, Shanghai, China

²Department of Physiology, University of Oklahoma Health Sciences Center, Oklahoma City, Oklahoma, United States

³Department of Ophthalmology, Xiangya Hospital, Central South University, Changsha, China

Correspondence: Jian-xing Ma, University of Oklahoma Health Sciences Center, 941 Stanton L. Young Boulevard, BSEB 328B, Oklahoma City, OK 73104, USA;

jian-xing-ma@ouhsc.edu.

Xun Xu, Department of Ophthalmology, Shanghai First People's Hospital, Shanghai JiaoTong University, 100 Haining Road, Shanghai, China, 200080;

drxxun@sjtu.edu.cn.

Submitted: October 7, 2013

Accepted: May 10, 2014

Citation: Wang Z, Moran E, Ding L, Cheng R, Xu X, Ma J-X. PPAR α regulates mobilization and homing of endothelial progenitor cells through the HIF-1 α /SDF-1 pathway. *Invest Ophthalmol Vis Sci.* 2014;55:3820-3832. DOI:10.1167/iovs.13-13396

PURPOSE. The mechanism for the antiangiogenic activity of peroxisome proliferator-activated receptor alpha (PPAR α) remains incompletely understood. Endothelial progenitor cells (EPC) are known to participate in neovascularization (NV). The purpose of this study was to investigate whether PPAR α regulates EPC during retinal NV.

METHODS. Retinal NV was induced by oxygen-induced retinopathy (OIR). Mice with OIR were injected intraperitoneally with the PPAR α agonist fenofibric acid (FA) or with adenovirus expressing PPAR α (Ad-PPAR α). Flow cytometry was used to quantify circulating and retinal EPC. Serum stromal cell-derived factor 1 (SDF-1) levels were measured by ELISA. Hypoxia was induced in primary human retinal capillary endothelial cells (HRCEC) and mouse brain endothelial cells (MBEC) by CoCl₂. Levels of SDF-1 and hypoxia-inducible factor 1 alpha (HIF-1 α) were measured by Western blotting.

RESULTS. Fenofibric acid and overexpression of PPAR α attenuated the increase of circulating and retinal EPC, correlating with suppressed retinal NV in OIR mice at P17. The PPAR α knockout enhanced the OIR-induced increase of circulating and retinal EPC. Fenofibric acid decreased retinal HIF-1 α and SDF-1 levels as well as serum SDF-1 levels in the OIR model. In HRCEC, PPAR α inhibited HIF-1 α nuclear translocation and SDF-1 overexpression induced by hypoxia. Further, MBEC from PPAR α ^{-/-} mice showed more prominent activation of HIF-1 α and overexpression of SDF-1 induced by hypoxia, compared with the wild-type (WT) MBEC. PPAR α failed to block SDF-1 overexpression induced by a constitutively active mutant of HIF-1 α , suggesting that regulation of SDF-1 by PPAR α was through blockade of HIF-1 α activation.

CONCLUSIONS. Peroxisome proliferator-activated receptor alpha suppresses ischemia-induced EPC mobilization and homing through inhibition of the HIF-1 α /SDF-1 pathway. This represents a novel molecular mechanism for PPAR α 's antiangiogenic effects.

Keywords: neovascularization, endothelial progenitor cells, PPAR α , oxygen-induced retinopathy, retina

Neovascularization (NV) refers to new blood vessel formation which includes two processes: angiogenesis and vasculogenesis. Asahara et al.¹ demonstrated that new blood vessels can form in the adult not only by the sprouting of fully differentiated endothelial cells (EC) (angiogenesis), but also by the participation of endothelial progenitor cells (EPC), independent of the pre-existing vasculature (vasculogenesis).¹ Bone marrow-derived EPC can differentiate into EC, and thus contribute to NV under multiple pathological conditions.² Similar to many stem cells, EPC have not been conclusively defined by specific cell surface markers.³ However, it has been well established that EPC express both stem cell antigens (CD117[c-kit] or CD34) and EC markers (Tie-2 or VEGFR2), which are commonly used to identify EPC.⁴

The trafficking of circulating EPC to hypoxic areas is still poorly understood. It has been suggested that vasculogenesis includes three steps: EPC mobilization from the bone marrow to the peripheral blood; homing/recruitment to the ischemic tissues; and differentiation into mature EC.⁵ To date, a well-accepted hypothesis is that the chemokine stromal cell-derived factor-1 (SDF-1 or CXCL12) and its main receptor CXCR4

expressed on progenitor cells^{6,7} play a pivotal role in EPC mobilization and homing.⁸ Stromal cell-derived factor 1 was initially identified in bone marrow stromal cells and functions to retain progenitor cells in the bone marrow under normal conditions.⁹ Under ischemic conditions, however, the SDF-1 level is upregulated in the blood, which reverses the bone marrow/blood SDF-1 gradient and thus increases the mobilization of EPC from the bone marrow to the blood. Similarly, SDF-1 expression is induced by hypoxia in ischemic/target tissues and attracts EPC homing to the desired sites.⁸ Further, Ceradini et al.¹⁰ established that SDF-1 gene expression is regulated by the transcription factor hypoxia-inducible factor-1 (HIF-1), and HIF-1 upregulates expression of SDF-1 in ischemic tissues in response to reduced oxygen tension. These findings suggest that HIF-1-mediated SDF-1 overexpression in an ischemic tissue and in the blood orchestrate EPC mobilization into the circulation and homing into the target tissue.

Retinopathy of prematurity (ROP) is a blinding disease in which retinal ischemia results in pathological retinal NV and impairment of retinal structure and function.¹¹ Oxygen-induced

retinopathy (OIR) is a commonly used animal model to study the pathogenesis of ischemia-induced retinal NV as found in ROP.¹² Previous studies have demonstrated that EPC mobilization participates in retinal NV in the OIR model.^{13,14} However, the regulatory mechanism for EPC trafficking under hypoxia remains unknown in OIR.

The peroxisome proliferator-activated receptor α (PPAR α) agonist fenofibrate and its bioactive metabolite fenofibric acid (FA) have been widely used for the treatment of dyslipidemia.¹⁵ Recent studies found that PPAR α also suppressed tumor growth and pathological NV.¹⁶ Our previous study demonstrated that intravitreal injection of fenofibrate significantly reduced retinal NV in a rat OIR model.¹⁷ Recently, Benameur et al.¹⁸ found that PPAR α is essential for microparticle-induced differentiation of EPC¹⁸; however, the direct regulatory role of PPAR α in EPC trafficking in vasculogenesis has not been documented.

We postulated that PPAR α might play a vital role in regulating the mobilization and homing of EPC to the retina under ischemia stress. In the present study, we evaluated the effects of PPAR α activation and overexpression on ischemia-induced EPC mobilization and homing using the OIR model. We also investigated the interactions between PPAR α and the HIF-1 α /SDF-1 axis and the role of these interactions in EPC trafficking.

MATERIALS AND METHODS

Animals

We purchased C57BL/6J (wild-type [WT]) and PPAR α ^{-/-} mice from Jackson Laboratory (Bar Harbor, ME, USA). All mice were maintained in a 12-hour light-dark cycle. All processes including care, use, and treatment of the animals were in strict agreement with the ARVO Statement for the Use of Animals in Ophthalmic and Vision Research and Guidelines for Animal Care and Use dictated by the University of Oklahoma Health Sciences Center.

OIR Model and FA or Ad-PPAR α Administration

The OIR model was induced in C57BL/6J mice and PPAR α ^{-/-} mice as described previously.¹² Briefly, mice were exposed to 75% oxygen from postnatal day (P)7 to P12 and subsequently returned to room air. Fenofibric acid (AKSci, Union City, CA, USA) was dissolved in dimethyl sulfoxide (DMSO) and injected intraperitoneally (10 mg/kg), once a day, from P12 to P17 ($n \geq 6$ for each group), with the same volume of DMSO as a vehicle control.

Adenovirus expressing PPAR α (Ad-PPAR α) was generated from the full-length human PPAR α cDNA (accession number NM_001001928; GeneCopeia, Rockville, MD, USA). Adenovirus-expressing green fluorescent protein (GFP) was used as control virus. The viruses were injected intraperitoneally (2.5×10^7 /mouse) at P12. Mice were euthanized at P17 and the whole blood, bone marrow, and retinas were collected for the following experiments.

To avoid the possible influence of circadian regulation of EPC trafficking and PPAR α function, all the procedures including intraperitoneal injection and animal euthanasia were performed at 10 AM.

Retinal Angiography and Quantification of Preretinal Vascular Cells

Mice at P17 were anesthetized and perfused with 50 mg/mL high-molecular weight FITC-dextran (2×10^6 ; Sigma-Aldrich,

St. Louis, MO, USA) as described by Smith et al.¹⁹ The retinas were dissected and flat-mounted, and the vasculature was then examined with a fluorescence microscope (CKX41; Olympus, Center Valley, PA, USA) by an operator masked to treatment allocation. Paraffin-embedded eyes were stained with hematoxylin and eosin to quantify the preretinal vascular cells as described previously.²⁰

Fluorescence-Activated Cells Sorter Analysis (FACS)

Circulating and retinal EPC were quantified by FACS. Fresh whole blood was collected from the left ventricular; and the retinas were dissected and digested with trypsin to generate single cell suspension. Mononuclear cells isolated from the whole blood (WB-MNC) or retina (retinal-MNC) were incubated with FITC-conjugated anti-mouse CD117 (c-kit); PE-conjugated anti-mouse CD202b (Tie-2); Brilliant Violet 421-conjugated anti-mouse CD34, PerCP/Cy5.5-conjugated anti-mouse CD309 (VEGFR2, Flk-1); and PE/Cy7-conjugated anti-mouse CD184 (CXCR4) antibodies (Biolegend, San Diego, CA, USA). After incubation, cells were fixed overnight in 1% paraformaldehyde. Data were acquired using a flow cytometer (S1000Ex; Stratigigm, San Jose, CA, USA) and analyzed using commercial software (CellCapTure v2.0; Stratigigm). A total of 20,000 monocytes were analyzed per sample, and the number of c-kit⁺/Tie2⁺ or CD34⁺/VEGFR2⁺ cells was counted and quantified as EPC.

Retina Trypsin Digestion

Trypsin digestion protocol to expose the retinal vasculature was performed as previously described.²¹ The retinas were dissected and fixed in 4% paraformaldehyde, followed by an overnight wash of distilled water. Then the retinas were incubated in a solution of 3% trypsin (Difco 1:250) in 0.1 M Tris buffer (pH 7.8) at 37°C for 1 hour. Other retina tissue except vasculature was carefully removed by gently patting and PBS washing. The generated retinal vasculature was subjected to immunostaining using the following primary antibodies: anti-CD31 (R&D, Minneapolis, MN, USA), anti-HIF-1 α and anti-SDF1 antibodies (Novus Biologicals, Littleton, CO, USA). AlexaFluor 647-AffiniPure Donkey Anti-Rabbit IgG and Alexa Fluor 488-AffiniPure Donkey Anti-goat IgG (Jackson ImmunoResearch Laboratory, Inc., West Grove, PA, USA) were used as secondary antibodies.

Cell Culture

Primary human retinal capillary endothelial cells (HRCEC) were purchased from Cell Systems (Kirkland, WA, USA), and cultured in Endothelial Cell Growth Medium MV with endothelial cell growth supplement (PromoCell, Heidelberg, Germany). Primary mouse brain endothelial cells (MBEC) were isolated from 21-day-old WT or PPAR α ^{-/-} mice and cultured as described by Wu et al.²² Cells of passages 2 to 6 were used for experiments. Cells were serum-starved in basal medium plus 0.5% fetal bovine serum (FBS) 8 hours before any treatment to synchronize. Hypoxia was induced by exposure of the cells to cobalt chloride (CoCl₂, 0.1 mM). Adenovirus expressing a constitutively active mutant of HIF-1 α , Ad-CA5, was a gift from Gregg Semenza, PhD, at Johns Hopkins University.²³ Adenovirus-expressing PPAR α was used to overexpress PPAR α , and Ad-GFP was used as control virus. All viruses were used at an MOI of 50.

Western Blot Analysis

Western blot analysis was performed to measure protein levels as described previously.²⁴ Antibodies for HIF-1 α and SDF-1

(Novus Biologicals) were used at 1:1000 dilution. The antibody for β -actin (Sigma-Aldrich) was used at 1:5000 dilution. The antibody for fibrillarlin (C13C3; Cell Signaling Technology, Danvers, MA, USA) was used at 1:1000 dilution.

Quantitative Real-Time RT-PCR

Total RNA was extracted using an RNA extraction kit (RNAeasy; Qiagen, Valencia, CA, USA). The following primers were used for quantitative real-time RT-PCR: human SDF-1 (forward): 5'-GTGTCAGTGGCGACACGTAG-3'; (reverse): 5'-TCCCATCCCACAGAGAGAAG-3', human β -actin (forward): 5'-GCCGATCCACACGGAGTACT-3'; (reverse): 5'-CTGGCACCCAGCACAAATG-3'. Polymerase chain reaction products were quantified as described previously.¹⁰

Immunohistochemistry

Frozen retinal sections (10 μ m) or cells were immunostained with indicated antibodies, and the nuclei were counterstained with DAPI (Vector Laboratories; Burlingame, CA, USA). The sections or slides were then viewed under a fluorescence microscope (Olympus). We used Anti-HIF-1 α and anti-SDF-1 antibodies (Novus Biologicals) as primary antibodies. Alexa-Fluor 647-AffiniPure Donkey Anti-Rabbit IgG (Jackson ImmunoResearch Laboratory, Inc.) was used as the secondary antibody.

Statistical Analysis

Quantitative data were expressed as mean \pm SEM. Data were analyzed with an unpaired two-tailed Student's *t*-test or ANOVA. Values (*P*) less than 0.05 were considered to be statistically significant.

RESULTS

FA Alleviates Retinal NV in OIR Mice

To determine if the PPAR α agonist FA suppressed ischemia-induced retinal NV, OIR mice were treated with FA from P12 to P17. Fluorescein angiography at P17 demonstrated severe NV in the flat-mounted retinas in the vehicle-treated OIR group compared with normoxia mice, and the FA-treated OIR group displayed alleviated retinal NV (Figs. 1A–F). The FA-treated OIR group developed significantly fewer preretinal vascular cells, in comparison with vehicle-treated OIR mice (Figs. 1G–I), supporting an inhibitory effect of FA on ischemia-induced retinal NV.

FA Attenuates Aberrant Increases of Circulating EPC in OIR Mice

Two pairs of well-accepted cell surface markers CD34/VEGFR2 and c-kit/Tie-2 were used to identify EPC population in the blood.⁴ As shown in Figures 2A through 2D, numbers of circulating EPC were considerably increased in the vehicle-treated OIR group, compared with normoxic mice, while FA treatment diminished the EPC increase. However, no significant change was found in the number of bone marrow EPC in normoxia, OIR, and FA-treated OIR groups (Supplementary Figs. S1A, S1B), suggesting that neither the OIR procedure nor the FA administration influences bone marrow EPC levels. Additionally, the same treatment of FA did not change circulating EPC numbers in normal mice at P17 (Supplementary Figs. S1C, S1D), indicating that FA has no effects on EPC mobilization under normal conditions.

Inhibitory Effect of FA on EPC Mobilization in the OIR Model is PPAR α -Dependent

To investigate whether the inhibitory effect of FA on EPC mobilization was through a PPAR α -dependent mechanism, we employed PPAR α ^{-/-} mice. Under normoxia, there was no significant difference in circulating EPC numbers between WT and PPAR α ^{-/-} mice at P17 (Fig. 2E). However, PPAR α ^{-/-} mice with OIR showed significantly more EPC in the blood, compared with WT mice with OIR at P17 (Fig. 2E). Furthermore, the FA treatment failed to decrease circulating EPC in PPAR α ^{-/-} mice with OIR (Fig. 2F), suggesting that FA's inhibitory effect on EPC mobilization in OIR was PPAR α -dependent.

To further confirm the effect of PPAR α on EPC, Ad-PPAR α (2.5×10^7 /mouse) were injected intraperitoneally into both OIR and normoxic mice at P12, with the same titer of Ad-GFP as control. The trypsin-digested retinas showed GFP expression in retinal vascular cells at P17, partly colocalized with the EC marker CD31 (Supplementary Fig. S4), indicating systemic administration of adenovirus-mediated gene expression in retina EC. Mice with OIR injected with Ad-PPAR α showed significantly decreased circulating EPC in comparison with Ad-GFP-injected OIR mice (Fig. 2G), demonstrating that PPAR α overexpression alone is sufficient to block OIR-induced EPC mobilization.

FA Inhibits Hypoxia-Induced Retinal EPC Increase in a PPAR α -Dependent Manner

To measure the effect of FA on EPC homing to the retina, the retinas were dissected and digested to generate single cell suspension. The retinal cells were stained with anti-CD34 and anti-VEGFR2 antibodies, and analyzed by FACS to determine EPC numbers in the retina. Numbers of EPC were increased in both of the retinas in WT and PPAR α ^{-/-} mice with OIR compared with the normoxia control (Fig. 2H). While there was no significant difference in retinal EPC numbers between PPAR α ^{-/-} and WT mice under normoxia conditions, consistent with circulating EPC numbers, PPAR α ^{-/-} OIR mice showed more prominent increases in retinal EPC, compared to WT OIR mice (Fig. 2H). Fenofibric acid dramatically down-regulated retinal EPC in WT OIR mice, but not in PPAR α ^{-/-} OIR mice, compared to OIR-vehicle treated groups; suggesting that PPAR α knockout abolished the effect of FA on EPC homing (Fig. 2H).

Moreover, Ad-PPAR α was employed to verify the effect of PPAR α on EPC homing. FACS results showed that Ad-PPAR α successfully inhibited the OIR-induced increase of CD34⁺/VEGFR2⁺ cells in the retina, confirming the essential role of PPAR α in regulating EPC homing to the retina under hypoxia condition.

FA Decreases CXCR4-Positive EPC in the Circulation and in the Retina

The SDF-1 receptor CXCR4 is widely expressed on stem cells and progenitor cells, and allows SDF-1 to recruit bone marrow cells to ischemic tissues.⁶ Our data showed that CXCR4⁺ cells can be detected in WB-MNC (Fig. 3A) and constitute nearly 90% of circulating CD34⁺/VEGFR2⁺ cells (Fig. 3B), indicating that CXCR4 is highly expressed on EPC in the circulation of the OIR model. As shown in Figure 3C and D, OIR mice developed significantly more CD34⁺/VEGFR2⁺/CXCR4⁺ cells in the circulation and in the retina, suggesting SDF-1/CXCR4 axis is involved in hypoxia-induced EPC mobilization and homing. Fenofibric acid decreased numbers of CD34⁺/VEGFR2⁺/CXCR4⁺ cells in the circulation and retina of OIR mice,

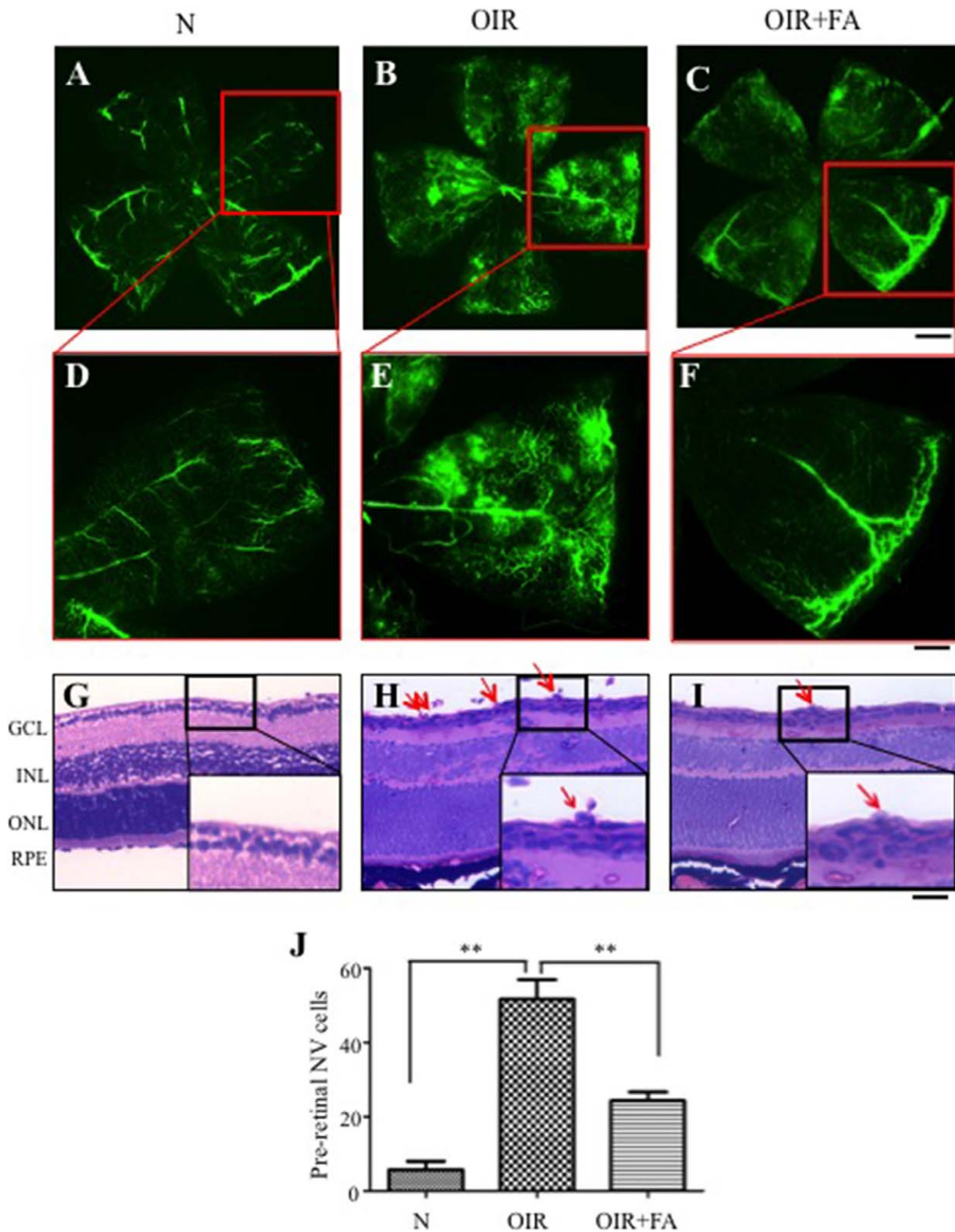


FIGURE 1. Effects of systemic administration of FA on retinal NV in OIR mice. Fenofibric acid was injected intraperitoneally into OIR mice (10 mg/kg/d) and normal mice (N) from P12 to P17, with the same volume of vehicle into the control group. (A-F) Representative images of fluorescein angiographs of retinal flat mounts at P17. Scale bars: 100 μ m (A-C), 40 μ m (D-F). (G-I) Representative retinal sections from mice at normoxia (G), vehicle-treated OIR mice (H), and FA-treated OIR mice (I). Red arrows indicate preretinal vascular cells. GCL, ganglion cell layer; INL, inner nuclear layer; ONL, outer nuclear layer. Scale bar: 40 μ m. (J) Quantification of preretinal vascular cells in eight noncontinuous sections per eye. ** $P < 0.01$ versus control, $n = 6$.

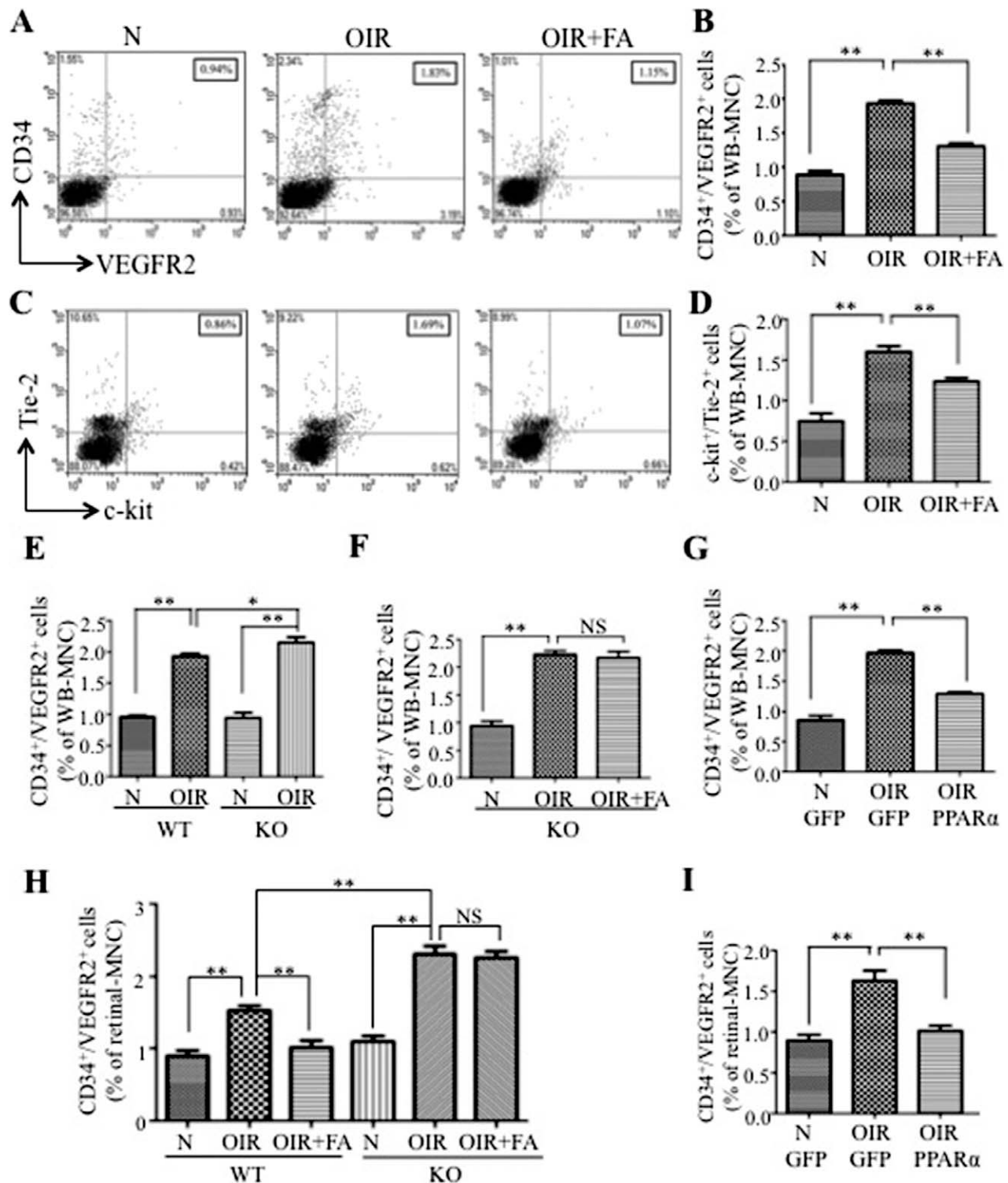


FIGURE 2. Reduction of aberrant EPC mobilization and homing by PPAR α in OIR mice. Fresh blood cells were collected from OIR and normal control mice (N) at P17. Cell markers CD34/VEGFR2 and c-kit/Tie-2 were labeled and analyzed by FACS to identify the EPC population. (A) Representative dot plots from FACS analysis. Double positive cells (CD34⁺/VEGFR2⁺) in the *right-upper quadrant* were considered to be EPC. The numbers in the boxes show percentage of EPC in WB-MNC. (B) Percentages of circulating CD34⁺/VEGFR2⁺ cells in WB-MNC from normal mice (N), OIR mice injected with vehicle (OIR), and OIR injected with FA (OIR + FA). (C) Representative dot plots from FACS analysis showing c-kit⁺/Tie-2⁺ cells in WB-MNCs. (D) Quantification of circulating c-kit⁺/Tie-2⁺ cells in WB-MNC. (E) Cells CD34⁺/VEGFR2⁺ in the blood compared between WT and PPAR α ^{-/-} (KO) mice under normoxia (N) and with OIR. (F) Mice (PPAR α ^{-/-} [KO]) mice with OIR were treated with FA from P12 to P17. Cells CD34⁺/VEGFR2⁺ were quantified at P17 and expressed as percentage of WB-MNC. (G) Wild-type mice with OIR were injected with Ad-PPAR α (2.5×10^7 /mouse) at P12, with Ad-GFP (2.5×10^7 /mouse) as control. Circulating CD34⁺/VEGFR2⁺ cells were quantified at P17. (H) Wild-type and KO mice (normal and OIR) were treated with FA, and percentages of CD34⁺/VEGFR2⁺ cells in the retina were determined by FACS (I) Wild-type mice with OIR were injected with Ad-PPAR α or Ad-GFP (2.5×10^7 /mouse) at P12, and retinal CD34⁺/VEGFR2⁺ cells were quantified at P17. Values represent mean \pm SEM ($n = 6$). ** $P < 0.01$ versus control. * $P < 0.05$ versus control. NS, not significant.

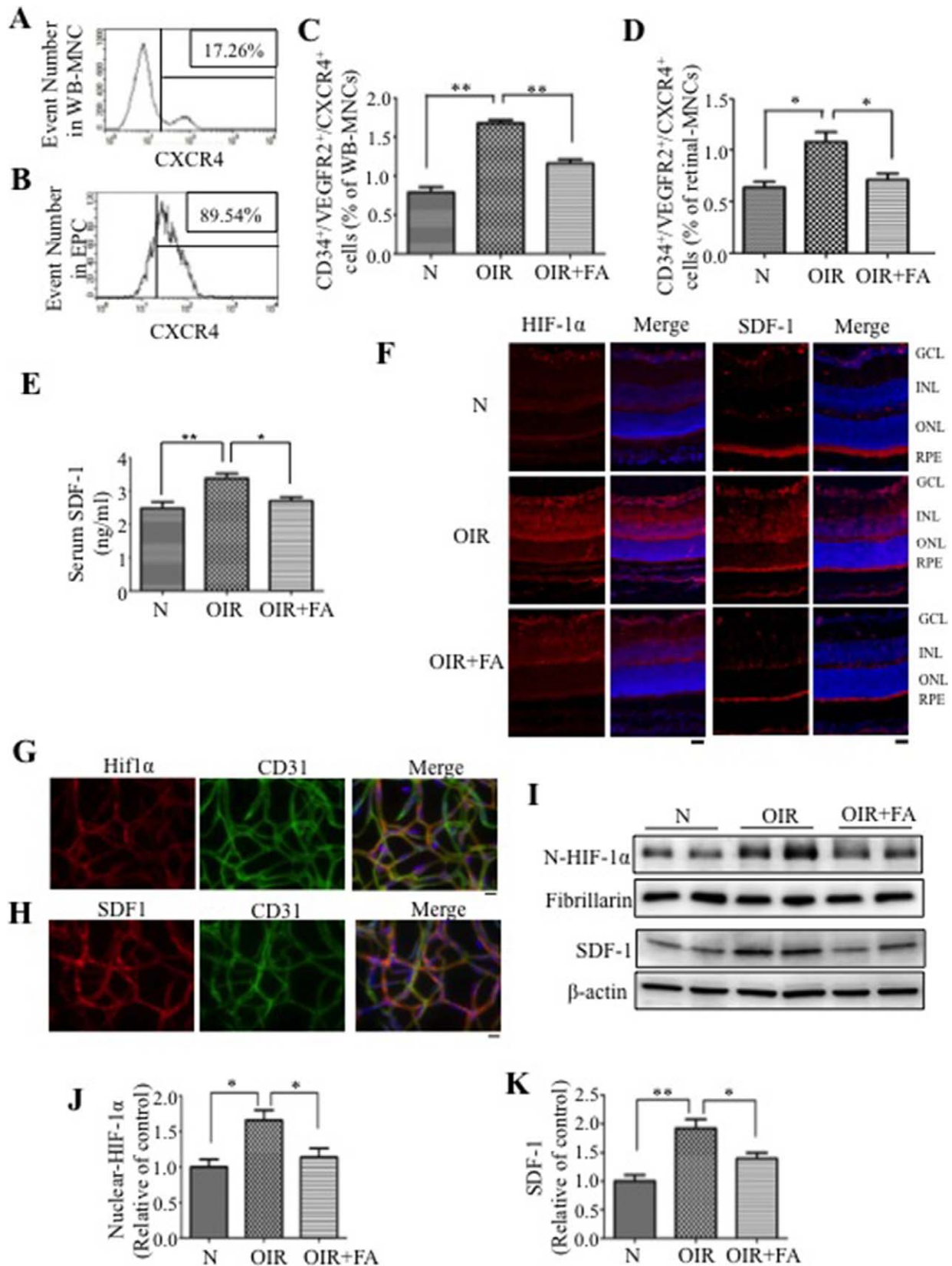


FIGURE 3. Fenofibric acid downregulates HIF-1 α and SDF-1 levels in OIR mice. (A, B) Histograms of CXCR4⁺ cells in WB-MNC (A) and in CD34⁺/VEGFR2⁺ cells (EPC) (B) in untreated OIR mice at P17, and numbers in the boxes denote percent cells. (C, D) Percentage of CXCR4⁺ EPC (CXCR4⁺/CD34⁺/VEGFR2⁺) in the circulation (C) and retina (D) in normal mice (N), OIR mice injected with vehicle (OIR), and OIR injected with FA (OIR + FA). (E) Serum SDF-1 levels in the same allocated groups measuring by ELISA. (F) Immunostaining (red) of HIF-1 α and SDF-1 in the retinas from normal mice (N), OIR mice treated with vehicle (OIR) and OIR mice treated with FA (OIR + FA). The nuclei were counterstained with DAPI (blue).

Scale bar: 20 μ m. (G, H) Immunohistochemistry of trypsin-digested retinas showing double staining of HIF-1 α (red) with CD31 (green [G]); and SDF-1 (red) with CD31 (green [H]) in untreated OIR mice. The nuclei were counterstained with DAPI (blue). Scale bar: 10 μ m. (I) Western blot analysis of nuclear HIF-1 α and total SDF-1 levels in the retina. (J, K) Semiquantification of nuclear HIF-1 α (J) and total SDF-1 (K) levels by densitometry. HIF-1 α was normalized by fibrillarlin, and SDF-1 was normalized by β -actin levels. Values represent mean \pm SEM ($n = 6$). ** $P < 0.01$ versus control. * $P < 0.05$ versus control.

compared with OIR mice treated with the vehicle (Figs. 3C, 3D), indicating that FA may function through suppressing EPC mobilization and homing by inhibiting the SDF-1/CXCR4 axis.

FA Downregulates the Serum SDF-1 Level and Suppresses HIF-1 α and SDF-1 Overexpression in the Retina

The HIF-1 α /SDF-1/CXCR4 axis has been shown to induce mobilization of EPC,¹⁰ and our data showed changes in circulating CXCR4⁺ EPC in the OIR model, suggesting a potential role of the SDF-1 in the EPC mobilization in the OIR model (Fig. 3C). Therefore, we measured the serum SDF-1 levels in OIR model. Our data showed that OIR induced serum SDF-1 level elevation, and FA reduced serum SDF-1 levels in OIR mice, compared with the vehicle control group (Fig. 3E), demonstrating a regulatory role of FA in bone marrow/blood SDF-1 gradient.

The HIF-1 α /SDF-1/CXCR4 axis has also been shown to participate in regulating EPC homing,⁸ and in consistent, our data also demonstrated the increased retinal CXCR4⁺ EPC in the OIR model (Fig. 3D). Furthermore, immunohistochemistry staining showed that retinal HIF-1 α and SDF-1 levels were significantly elevated in OIR mice, compared with those in normoxia control, while FA attenuated these increases in the OIR retina (Fig. 3F). Further, HIF-1 α and SDF-1 were colocalized with CD31 in the retinal vasculature, suggesting that HIF-1 α /SDF-1 response in OIR occurred in retinal EC (Figs. 3G, 3H). Western blot analysis also confirmed that HIF-1 α and SDF-1 protein levels were significantly increased in OIR retinas, which was reversed by FA treatment (Figs. 3I–K). Taken together, HIF-1 α and SDF-1 levels are increased in OIR retinas and downregulated by the PPAR α agonist FA.

PPAR α Inhibits Hypoxia-Induced SDF-1 Expression In Vitro

To study the mechanism by which FA regulates SDF-1 expression, HRCEC were exposed to CoCl₂, a known HIF-1 α activator, to simulate the hypoxic stress. As shown in Figures 4A through 4D, exposure of HRCEC to 0.1 mM CoCl₂ induced significant SDF-1 upregulation, compared with the sodium chloride (NaCl)-treated group (control group). Fenofibric acid prevented hypoxia-induced SDF-1 overexpression in a concentration-dependent manner (Figs. 4A, 4B). Likewise, PPAR α overexpression by Ad-PPAR α infection resulted in significant suppression of hypoxia-induced SDF-1 expression (Figs. 4C, 4D). As shown by real-time RT-PCR, the SDF-1 mRNA increased by 4- to 5-fold after exposure to CoCl₂, while FA and Ad-PPAR α both blocked the hypoxic induction of SDF-1, suggesting that PPAR α regulates SDF-1 expression at the transcriptional level (Figs. 4E, 4F).

PPAR α Blocks Hypoxia-Induced HIF-1 α Nuclear Translocation

Western blot analysis showed that FA and Ad-PPAR α significantly attenuated CoCl₂-induced HIF-1 α accumulation in whole cell lysates and nuclear extracts (Figs. 5A–D). To further verify the blockade of HIF-1 α nuclear translocation by PPAR α , we

stained HRCEC with an anti-HIF-1 α antibody. The results showed that 25 μ M FA and Ad-PPAR α both successfully attenuated CoCl₂-induced HIF-1 α nuclear translocation (Figs. 5E, 5F).

PPAR α is an Endogenous Inhibitor of HIF-1 α Activation and SDF-1 Expression

To determine the impacts of PPAR α deficiency on SDF-1 expression and HIF-1 α activation, MBEC were isolated and cultured from WT and PPAR α ^{-/-} mice following a documented protocol.²² Western blot analysis showed that CoCl₂ induced more prominent elevation of HIF-1 α and SDF-1 levels in PPAR α ^{-/-} MBEC than in WT MBEC, while there was no significant difference in the levels of HIF-1 α and SDF-1 between WT and PPAR α ^{-/-} MBEC in normal conditions (Figs. 6A–C). Consistent with the results in HRCEC, FA decreased HIF-1 α and SDF-1 in WT MBEC but not in PPAR α ^{-/-} MBEC under hypoxic conditions, suggesting that PPAR α knockout abolished the regulatory effect of FA on SDF-1 and HIF-1 α (Figs. 6A–C).

PPAR α Inhibits Hypoxia-Induced SDF-1 Expression by Suppressing HIF-1 α

To determine whether the negative regulation of PPAR α on hypoxia-induced SDF-1 expression is through suppression of HIF-1 activity, we employed Ad-CA5, which expresses a constitutively active mutant of HIF-1 α independent of hypoxia.²³ As shown in Figures 6D through 6G, Ad-CA5-induced SDF-1 upregulation was not affected by either FA or Ad-PPAR α . Together, these data suggested that downregulation of SDF-1 expression induced by PPAR α is through blockade of HIF-1 α activation by hypoxia.

DISCUSSION

Endothelial progenitor cell mobilization and homing are both important processes in vasculogenesis and are implicated in pathological NV conditions, but their regulations are not completely understood.⁴ The present study demonstrates for the first time that PPAR α plays an important role in the regulation of EPC trafficking including mobilization and homing. Our results show that activation and overexpression of PPAR α both suppress the aberrant EPC mobilization and homing induced by hypoxia. Further, PPAR α deficiency resulted in more prominent increases of circulating EPC and retinal EPC under hypoxia condition. Our studies also identify that PPAR α suppresses hypoxia-induced EPC trafficking (i.e., inhibiting the HIF-1 α /SDF-1/CXCR4 axis), which has been shown to play a key role in EPC mobilization and homing.^{8,10,25} Our findings reveal a novel function of PPAR α in modulating EPC in vasculogenesis and suggest that PPAR α might be a potential therapeutic target for hypoxia-induced NV.

Until recently, the pathological generation of new blood vessels in the adult was thought to occur exclusively through angiogenesis, defined as the sprouting of vessels from existing capillaries.²⁶ However, Asahara et al.¹ discovered the existence of EPC, which permanently expanded our knowledge regarding pathological NV. The EPC participate in vasculogenesis in three steps: EPC mobilization from the

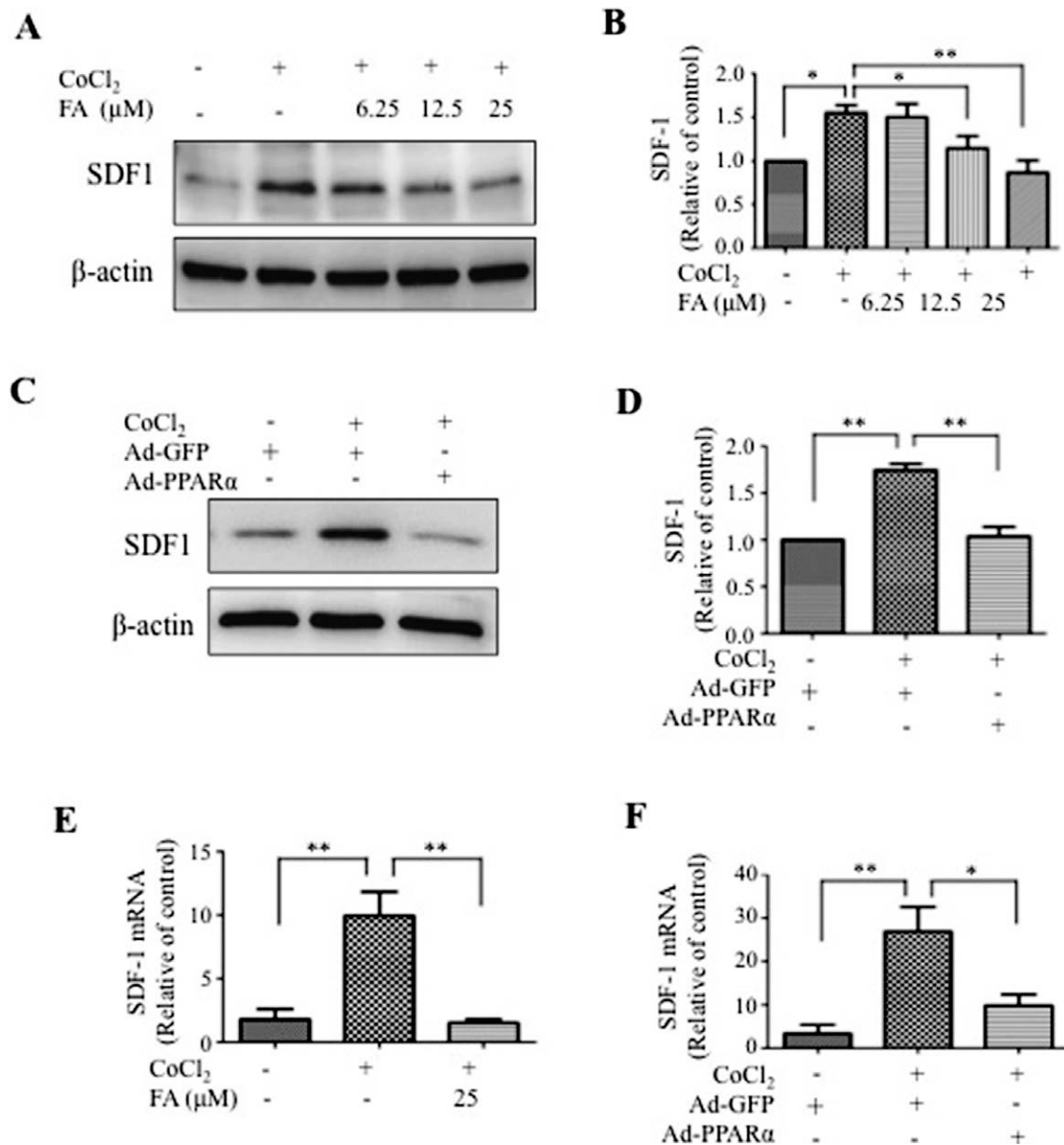


FIGURE 4. Receptor PPAR α inhibits hypoxia-induced SDF-1 expression in vitro. (A, B) Human retinal capillary endothelial cells were treated with various concentrations of FA as indicated for 24 hours and exposed to 0.1 mM CoCl₂ for 6 hours. The same amount of proteins from cell lysates was used for Western blot analysis. Levels of SDF-1 were semiquantified by densitometry, normalized by β -actin levels and expressed as relative to control. (C, D) Human retinal capillary endothelial cells were infected with Ad-PPAR α at MOI of 50 for 48 hours and exposed to CoCl₂ for another 6 hours. Levels of SDF-1 were measured by Western blot analysis, semiquantified by densitometry, normalized by β -actin levels and expressed as relative to control. (E, F) Human retinal capillary endothelial cells were treated with FA (24 hours) and Ad-PPAR α (48 hours) and exposed to 0.1 mM CoCl₂ for 6 hours. Expression levels of SDF-1 mRNA in cells treated with FA (E) and Ad-PPAR α (F) under hypoxia were quantified by real-time PCR and normalized by β -actin. Values represent mean \pm SEM ($n = 3$). ** $P < 0.01$ versus control. * $P < 0.05$ versus control.

bone marrow to the peripheral blood; homing/recruitment to the ischemic tissues; and EPC differentiation into mature EC, contributing the formation of new vessels in ischemic tissues.⁵ Endothelial progenitor cell-mediated revascularization could be beneficial for tissue repair under some conditions such as myocardial infarction.²⁷ However, under some pathological conditions in which blood vessel formation is detrimental—such as ROP, proliferative diabetic retinopathy and cancer^{13,28}—it is necessary to reduce or block abnormal EPC trafficking. Retinopathy of prematurity is caused by hypoxia-induced retinal NV and often leads to irreversible visual acuity loss. Previous studies have demonstrated that aberrant EPC mobilization plays a prominent role in ROP pathophysiology.²⁹

Recent studies reported that increased EPC mobilization contributes to retinal NV in the OIR model, a commonly used model for ROP.^{13,14} Our work also confirmed explicit increases of circulating EPC at P17 in OIR mice (Figs. 2A–G). Moreover, the present study demonstrated significant increases of retinal EPC at P17 in OIR mice as well (Figs. 2H–I). Therefore, OIR was used as a NV model to investigate the role of PPAR α in the regulation of EPC trafficking under hypoxia.

Nuclear receptor PPAR α is broadly expressed in various tissues, and exerts a wide spectrum of effects.³⁰ Peroxisome proliferator-activated receptor alpha was first recognized for its hypolipidemic effects, and PPAR α agonists are clinically used to treat hyperlipidemia/dyslipidemia.¹⁵ However, two

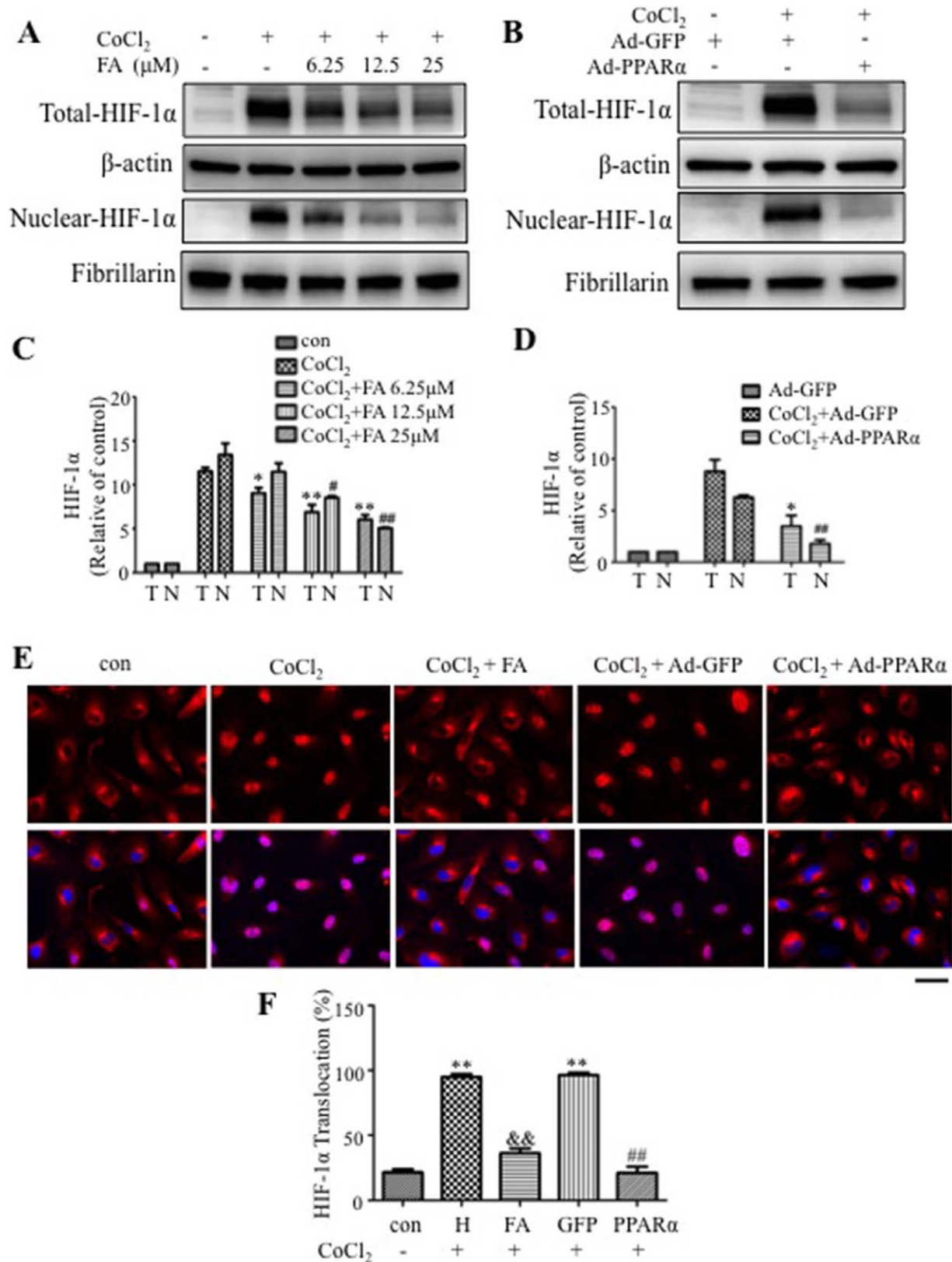


FIGURE 5. Receptor PPAR α blocks hypoxia-induced HIF-1 α activation. (A, C) Effect of FA on total and nuclear HIF-1 α levels in HRCEC under hypoxia. Human retinal capillary endothelial cells were treated with CoCl₂ and various concentrations of FA as indicated. Total (T) and nuclear (N) HIF-1 α levels were measured by Western blot analysis, semiquantified by densitometry and normalized by β -actin and fibrillarlin levels, respectively. The total and nuclear HIF-1 α levels were expressed as relative to control. (B, D) Effect of Ad-PPAR α on total and nuclear HIF-1 α levels. Human retinal capillary endothelial cells were infected with Ad-PPAR α (MOI = 50) for 48 hours and then exposed to CoCl₂ for 6 hours, with Ad-GFP as control. Levels of HIF-1 α levels were measured in total cell lysates and in nuclear extracts, semiquantified by densitometry, normalized by β -actin and

fibrillar levels, respectively, and expressed as relative to control. $**P < 0.01$. $*P < 0.05$ versus CoCl₂ + vehicle (C) or CoCl₂ + Ad-GFP (D) in total protein. $###P < 0.01$. $#P < 0.05$ versus CoCl₂ + vehicle (C) or CoCl₂ + Ad-GFP (D) in nuclear protein. (E) Immunohistochemistry showing nuclear translocation of HIF-1 α . Human retinal capillary endothelial cells were treated with 0.1 mM CoCl₂ for 6 hours, in the presence of pretreated 25 μ M FA, or infected with Ad-PPAR α for 48 hours. The cells were immunostained with an antibody for HIF-1 α (red), with the nucleus counterstained with DAPI (blue). Scale bar: 40 μ m. (F) Cells with HIF-1 α signal in the nuclei were quantified in five random fields per dish, averaged and expressed as percentage of total cells in the field. $**P < 0.01$ versus control. $&&P < 0.01$ versus CoCl₂ + vehicle. $###P < 0.01$ versus CoCl₂ + Ad-GFP. Values represent mean \pm SEM ($n = 3$).

independent, perspective clinical studies demonstrated that fenofibrate, a PPAR α agonist, has a potent therapeutic effect on diabetic retinopathy and other microvascular complications in type 2 diabetic patients.^{31,32} Our previous study demonstrated that fenofibrate ameliorates ischemia-induced retinal NV in a rat OIR model, but did not address its role in EPC regulation.¹⁷ In this study, we utilized both PPAR α agonist and overexpression of PPAR α to investigate its role in regulating EPC in the OIR model. We demonstrated that systemic administration of FA reduced circulating and retinal EPC in the OIR model, correlating with attenuated retinal NV in OIR mice (Figs. 1, 2). However, EPC numbers in the bone marrow were unchanged in OIR or OIR mice treated with FA (Supplementary Figs. S1A, S1B), suggesting that acute hypoxia and PPAR α activation affect EPC mobilization and homing but not bone marrow EPC generation. These findings suggest that the anti-NV effect of PPAR α is likely through blocking EPC trafficking from the bone marrow to ischemic tissue.

As shown by previous studies, PPAR α is directly involved in the control of clock genes expression, and the peak of PPAR α is at zeitgeber time 4 (ZT4).³³ Additionally, EPC release is circadian-regulated, and the peak is at ZT3-4.³⁴ Under some pathological circumstances, such as diabetes, the circadian regulation is lost.³⁴ However, there are no documented studies regarding circadian regulation of the EPC release in the OIR animals. We considered the impacts of the circadian cycle when we designed the experiments, and we performed intraperitoneal injections and euthanized animals at 10 AM (ZT4) for all of the experiments, to avoid the possible interference by the circadian cycle.

To determine if the effect of FA on EPC trafficking is through a PPAR α -dependent mechanism, we employed PPAR α ^{-/-} mice. Interestingly, our results showed that OIR induced significantly higher increases of circulating and retinal EPC in PPAR α ^{-/-} mice than in WT mice (Figs. 2E, 2H). In the absence of PPAR α , FA lost its inhibitory effect on the EPC increases in the circulation and in the retina (Figs. 2F, 2H), suggesting that the effect of FA on EPC mobilization and homing is PPAR α -dependent. Furthermore, systemic injection of Ad-PPAR α alone also suppressed aberrant circulating and retinal EPC in OIR, providing further evidence that PPAR α is responsible for the EPC regulation (Fig. 3C). On the other hand, activation of PPAR α by FA did not change the number of circulating EPC under normal conditions (Supplementary Figs. S1C, S1D), and there is no difference in the numbers of circulating and retinal EPC between WT and PPAR α ^{-/-} mice under normal conditions (Figs. 2E, 2H). We also observed that PPAR α ^{-/-} mice under constant normoxia displayed normal development of retinal vasculature at P17 compared with WT mice (Supplementary Fig. S3). These observations suggested that PPAR α exerts its protective functions only under stress conditions. Taken together, our data revealed a novel function of PPAR α in the modulation of EPC trafficking in ischemia.

Trafficking of EPCs is a highly regulated process, and SDF-1 has been shown to play an important role in EPC mobilization and homing to ischemic tissues.^{35,36} Stromal cell-derived factor 1 is widely expressed in multiple retinal cell types, including EC and retinal cells, and is overproduced under ischemia.

Under hypoxic conditions, SDF-1 is released from ischemic tissues into the circulation, leading to increased EPC mobilization and homing to generate new blood vessels.^{35,36} A previous report¹⁰ and our FACS data (Fig. 3B) both showed that almost 90% of circulating EPC expresses CXCR4, the main SDF-1 receptor, and CXCR4⁺ EPC are increased in the circulation and retina in OIR mice, and downregulated by FA treatment, indicating that the SDF-1/CXCR4 axis plays a crucial role in regulating EPC in the OIR model. To elucidate the mechanism by which PPAR α suppresses EPC mobilization and homing under hypoxia, the present study investigated the regulation of SDF-1. Results showed that SDF-1 was substantially increased in the OIR serum and retinas, while FA successfully inhibits the increases of serum and retinal SDF-1 levels (Figs. 3E, 3F, 3I). Since the SDF-1 response to hypoxia is likely EC specific (Fig. 3H), we studied the regulation of PPAR α on SDF-1 in retinal EC. In primary HRCEC, activation of PPAR α by FA and overexpression of PPAR α successfully suppressed CoCl₂-induced SDF-1 overexpression at the protein and mRNA levels (Fig. 4). Further, our studies using primary EC from PPAR α ^{-/-} mice showed that PPAR α knockout enhanced hypoxia-induced SDF-1 overexpression, compared with EC from WT mice, and FA lost its inhibitory effect on SDF-1 expression in PPAR α ^{-/-} EC, suggesting that PPAR α functions as an endogenous negative regulator of SDF-1 (Figs. 6A, 6C). These results provide the first evidence suggesting that PPAR α 's regulation of EPC is likely via downregulation of SDF-1 level.

There is no documented evidence suggesting that SDF-1 is a direct target gene of PPAR α , and the interactions between SDF-1 and PPAR α have not been established. To define the signaling pathway mediating the downregulation of SDF-1 expression by PPAR α , we measured the hypoxia indicator, HIF-1 α , which has been shown to regulate the transcription of SDF-1, and thus, to stimulate the trafficking of EPC under hypoxia.¹⁰ Zhou et al.²⁴ demonstrated that PPAR α suppresses HIF-1 α signaling by promoting HIF-1 α degradation in cancer cells. Consistently, our study found that in HRCEC, FA and Ad-PPAR α both inhibited hypoxia-induced HIF-1 α accumulation and prevented HIF-1 α nuclear translocation (Fig. 5). Moreover, primary MBEC from PPAR α ^{-/-} mice showed an enhanced HIF-1 α accumulation under hypoxia, compared with MBEC from WT mice (Figs. 6A, 6B). Similar to the observation in SDF-1, PPAR α knockout abolished the inhibitory effect of FA on HIF-1 α accumulation (Figs. 6A, 6B), further suggesting the FA's effect on HIF-1 α is through PPAR α . These observations confirmed the regulatory role of PPAR α in HIF-1 α accumulation, consistent with previous studies.²⁴

To determine whether PPAR α suppresses SDF-1 through HIF-1 α , we employed Ad-CA5, which expresses a constitutively active mutant of HIF-1 α , and lacks the oxygen-dependent degradation domain and is thus stabilized in normoxic conditions.²³ Our results showed that Ad-CA5 significantly induced SDF-1 expression under normoxia, and that neither FA nor Ad-PPAR α had any significant effect on SDF-1 overexpression induced by this constitutively active mutant of HIF-1 α (Figs. 6D-G), indicating that PPAR α -induced downregulation of SDF-1 expression is through attenuating HIF-1 α activation under hypoxia.

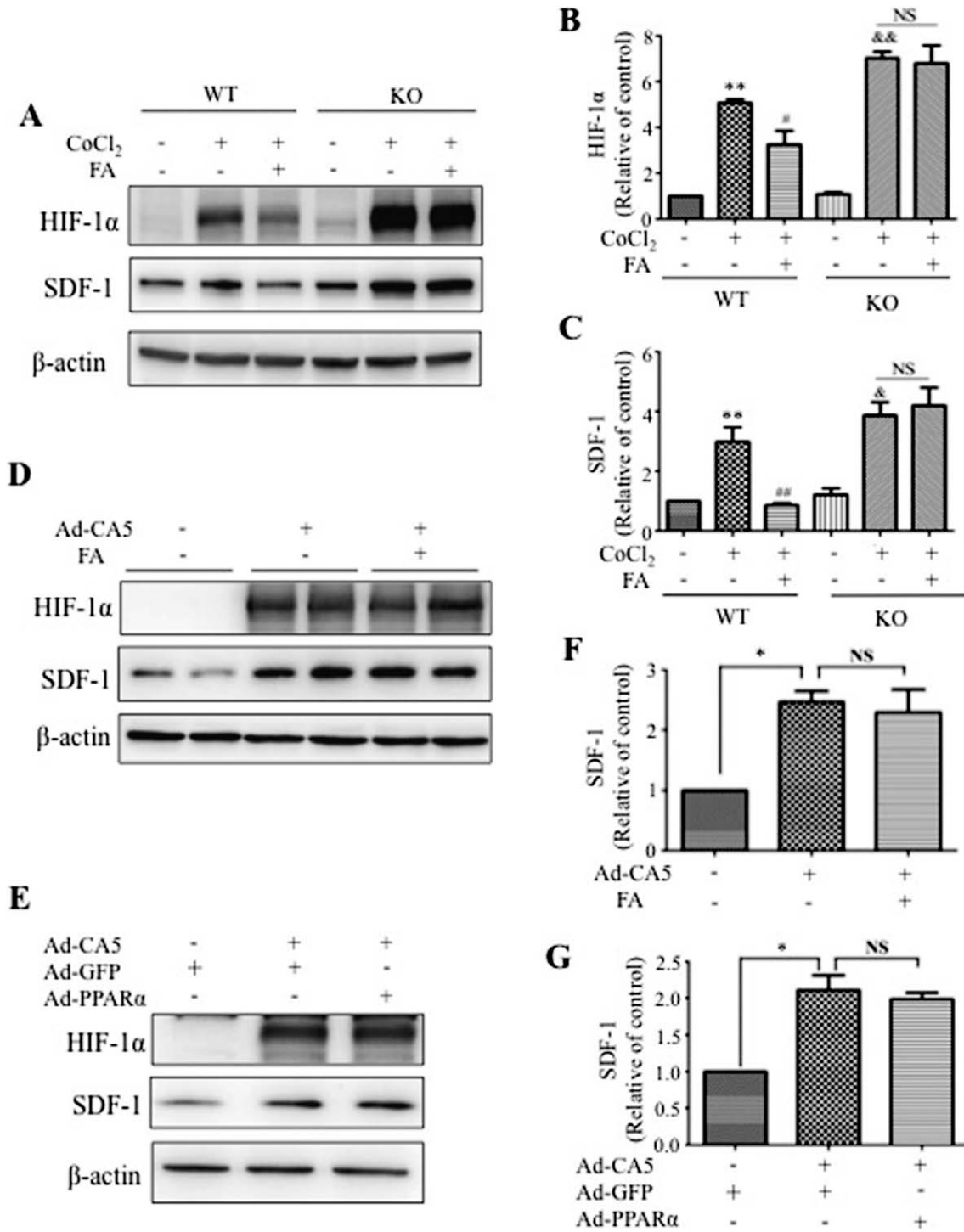


FIGURE 6. Mechanism for the effects of PPAR α on hypoxia-induced SDF-1 expression. (A) Mouse brain endothelial cells were isolated and cultured from WT and PPAR α ^{-/-} (KO) mice. The cells were treated with CoCl₂ for 6 hours following pretreatment with 25 μ M FA for 18 hours. Levels of HIF-1 α and SDF-1 were measured with Western blot analysis. (B, C) Semi-quantification of HIF-1 α (B) and SDF-1 (C) levels by densitometry and normalized by β -actin levels. ***P* < 0.01. **P* < 0.05 versus WT control. ##*P* < 0.01. #*P* < 0.05 versus WT CoCl₂ + vehicle. &&*P* < 0.01. &*P* < 0.05 versus KO control. (D) The effect of FA on SDF-1 expression induced by Ad-CA5. Human retinal capillary endothelial cells were infected with Ad-CA5 at MOI of 50 and treated with 25 μ M FA for 24 hours. Levels of HIF-1 α and SDF-1 were measured by Western blot analysis. (E) The effect of Ad-PPAR α on SDF-1 expression induced by Ad-CA5. Human retinal capillary endothelial cells were infected with Ad-PPAR α and Ad-CA5 at MOI of 50 for 48 hours. Adenovirus-expressing GFP was used as control. Levels of HIF-1 α and SDF-1 were measured by Western blot analysis. (F, G) Semiquantification of SDF-1 by densitometry and normalized by β -actin levels. Values represent mean \pm SEM (*n* = 3). ***P* < 0.01. **P* < 0.05 versus control (F) or Ad-GFP (G) group.

In summary, our work has identified PPAR α as a novel regulator of EPC mobilization and homing, and established the underlying molecular mechanism of the PPAR α action. However, some questions remain to be addressed. It is unclear why PPAR α knockout does not alter circulating and retinal EPC numbers under normal conditions, and if other signaling pathways could be involved in the regulation, since EPC trafficking is a multisignaling mediated, complicated process. For example, a previous study found that PPAR α upregulates Sphk1 and S1P in response to free fatty acids,³⁷ and S1P stimulates the functional capacity of progenitor cells by activating the CXCR4-dependent signaling pathway.³⁸ It remains to be studied how PPAR α interact with S1P in EPC regulation. Besides, HIF-1 induces numerous growth factors in addition to SDF-1, such as erythropoietin (EPO), and EPO is known to promote EPC mobilization from the bone marrow.^{39,40} Our data also showed that serum EPO is upregulated in OIR mice and inhibited by FA treatment (Supplementary Fig. S5), indicating that there are more than one mechanism involved in PPAR α regulating EPC trafficking. Future work will focus on the clinical studies of FA or other PPAR α agonists in ROP patients and mechanistic studies to delineate other signaling pathways mediating PPAR α 's effect on EPC mobilization and homing.

CONCLUSIONS

The present study demonstrates that PPAR α inhibits hypoxia-induced retinal NV at least in part through blocking the aberrant EPC mobilization and homing. This action is through inhibition of the HIF-1 α /SDF-1 pathway. These observations revealed a novel function of PPAR α in EPC regulation and novel interactions between PPAR α and SDF-1. These results suggest that PPAR α is a putative drug target for the modulation of EPC trafficking and pathological NV.

Acknowledgments

Supported by National Institutes of Health Grants EY018659, EY012231, EY019309, P20GM104934, and grants from the Oklahoma Center for the Advancement of Science and International Retinal Research Foundation (IRRF).

Disclosure: **Z. Wang**, None; **E. Moran**, None; **L. Ding**, None; **R. Cheng**, None; **X. Xu**, None; **J.-X. Ma**, None

References

- Asahara T, Murohara T, Sullivan A, et al. Isolation of putative progenitor endothelial cells for angiogenesis. *Science*. 1997; 275:964-967.
- Hill JM, Zalos G, Halcox JP, et al. Circulating endothelial progenitor cells, vascular function, and cardiovascular risk. *N Engl J Med*. 2003;348:593-600.
- Hirschi KK, Ingram DA, Yoder MC. Assessing identity, phenotype, and fate of endothelial progenitor cells. *Arterioscler Thromb Vasc Biol*. 2008;28:1584-1595.
- Patschan D, Krupinca K, Patschan S, Zhang Z, Hamby C, Goligorsky MS. Dynamics of mobilization and homing of endothelial progenitor cells after acute renal ischemia: modulation by ischemic preconditioning. *Am J Physiol Renal Physiol*. 2006;291:F176-F185.
- Urbich C, Dimmeler S. Endothelial progenitor cells: characterization and role in vascular biology. *Circ Res*. 2004;95:343-353.
- Peled A, Petit I, Kollet O, et al. Dependence of human stem cell engraftment and repopulation of NOD/SCID mice on CXCR4. *Science*. 1999;283:845-848.
- Peled A, Grabovsky V, Habler L, et al. The chemokine SDF-1 stimulates integrin-mediated arrest of CD34(+) cells on vascular endothelium under shear w. *J Clin Invest*. 1999; 104:1199-1211.
- Zhou X, Porter AL, Robinson DK, Shim MS, Guo Y. Nano-enabled drug delivery: A research profile [published online ahead of print March 12, 2014]. *Nanomedicine*. doi:10.1016/j.nano.2014.03.001.
- Kullberg M, McCarthy R, Anchordoquy TJ. Gene delivery to Her-2+ breast cancer cells using a two-component delivery system to achieve specificity [published online ahead of print March 12, 2014]. *Nanomedicine* doi:10.1016/j.nano.2014.03.001.
- Ceradini DJ, Kulkarni AR, Callaghan MJ, et al. Progenitor cell trafficking is regulated by hypoxic gradients through HIF-1 induction of SDF-1. *Nat Med*. 2004;10:858-864.
- Hartnett ME, Penn JS. Mechanisms and management of retinopathy of prematurity. *N Engl J Med*. 2012;367:2515-2526.
- Connor KM, Krahn NM, Dennison RJ, et al. Quantification of oxygen-induced retinopathy in the mouse: a model of vessel loss, vessel regrowth and pathological angiogenesis. *Nat Protoc*. 2009;4:1565-1573.
- Nakagawa Y, Masuda H, Ito R, et al. Aberrant kinetics of bone marrow-derived endothelial progenitor cells in the murine oxygen-induced retinopathy model. *Invest Ophthalmol Vis Sci*. 2011;52:7835-7841.
- Longeras R, Farjo K, Ihnat M, Ma JX. A PEDF-derived peptide inhibits retinal neovascularization and blocks mobilization of bone marrow-derived endothelial progenitor cells. *Exp Diabetes Res*. 2012;2012:518426.
- Kraja AT, Province MA, Straka RJ, Ordovas JM, Borecki IB, Arnett DK. Fenofibrate and metabolic syndrome. *Endocr Metab Immune Disord Drug Targets*. 2010;10:138-148.
- Zak Z, Gelebart P, Lai R. Fenofibrate induces effective apoptosis in mantle cell lymphoma by inhibiting the TNF α /NF- κ B signaling axis. *Leukemia*. 2010;24: 1476-1486.
- Chen Y, Hu Y, Lin M, et al. Therapeutic effects of PPAR α agonists on diabetic retinopathy in type 1 diabetes models. *Diabetes*. 2013;62:261-272.
- Benamer T, Tual-Chalot S, Andriantsitohaina R, Martinez MC. PPAR α is essential for microparticle-induced differentiation of mouse bone marrow-derived endothelial progenitor cells and angiogenesis. *PLoS One*. 2010;5:e12392.
- Smith LE, Wesolowski E, McLellan A, et al. Oxygen-induced retinopathy in the mouse. *Invest Ophthalmol Vis Sci*. 1994;35: 101-111.
- Chen Y, Hu Y, Zhou T, et al. Activation of the Wnt pathway plays a pathogenic role in diabetic retinopathy in humans and animal models. *Am J Pathol*. 2009;175:2676-2685.
- Lin CD, Kou YY, Liao CY, et al. Zinc oxide nanoparticles impair bacterial clearance by macrophages [published online ahead of print March 17, 2014]. *Nanomedicine (Lond)*. doi:10.2217/nmm.14.48.
- Wu Z, Hofman FM, Zlokovic BV. A simple method for isolation and characterization of mouse brain microvascular endothelial cells. *J Neurosci Methods*. 2003;130:53-63.
- Kelly BD, Hackett SF, Hirota K, et al. Cell type-specific regulation of angiogenic growth factor gene expression and induction of angiogenesis in nonischemic tissue by a constitutively active form of hypoxia-inducible factor 1. *Circ Res*. 2003;93:1074-1081.
- Zhou J, Zhang S, Xue J, et al. Activation of peroxisome proliferator-activated receptor α (PPAR α) suppresses hypoxia-inducible factor-1 α (HIF-1 α) signaling in cancer cells. *J Biol Chem*. 2012;287:35161-35169.
- Ratajczak MZ, Zuba-Surma E, Kucia M, Reza R, Wojakowski W, Ratajczak J. The pleiotropic effects of the SDF-1-CXCR4 axis in

- organogenesis, regeneration and tumorigenesis. *Leukemia*. 2006;20:1915-1924.
26. Folkman J, Shing Y. Angiogenesis. *J Biol Chem*. 1992;267:10931-10934.
 27. Fazel S, Cimini M, Chen L, et al. Cardioprotective c-kit+ cells are from the bone marrow and regulate the myocardial balance of angiogenic cytokines. *J Clin Invest*. 2006;116:1865-1877.
 28. Tsutsumi H, Tanaka T, Ohashi N, et al. Therapeutic potential of the chemokine receptor CXCR4 antagonists as multifunctional agents. *Biopolymers*. 2007;88:279-289.
 29. Machalinska A, Modrzejewska M, Kotowski M, et al. Circulating stem cell populations in preterm infants: implications for the development of retinopathy of prematurity. *Arch Ophthalmol*. 2010;128:1311-1319.
 30. Hiukka A, Maranghi M, Matikainen N, Taskinen MR. PPAR-alpha: an emerging therapeutic target in diabetic microvascular damage. *Nat Rev Endocrinol*. 2010;6:454-463.
 31. Keech AC, Mitchell P, Summanen PA, et al. Effect of fenofibrate on the need for laser treatment for diabetic retinopathy (FIELD study): a randomised controlled trial. *Lancet*. 2007;370:1687-1697.
 32. Accord Study Group, Accord Eye Study Group, Chew EY, et al. Effects of medical therapies on retinopathy progression in type 2 diabetes. *N Engl J Med*. 2010;363:233-244.
 33. Yang X, Downes M, Yu RT, et al. Nuclear receptor expression links the circadian clock to metabolism. *Cell*. 2006;126:801-810.
 34. Busik JV, Tikhonenko M, Bhatwadekar A, et al. Diabetic retinopathy is associated with bone marrow neuropathy and a depressed peripheral clock. *J Exp Med*. 2009;206:2897-2906.
 35. Hattori K, Heissig B, Tashiro K, et al. Plasma elevation of stromal cell-derived factor-1 induces mobilization of mature and immature hematopoietic progenitor and stem cells. *Blood*. 2001;97:3354-3360.
 36. De Falco E, Porcelli D, Torella AR, et al. SDF-1 involvement in endothelial phenotype and ischemia-induced recruitment of bone marrow progenitor cells. *Blood*. 2004;104:3472-3482.
 37. Ross JS, Hu W, Rosen B, Snider AJ, Obeid LM, Cowart LA. Sphingosine kinase 1 is regulated by peroxisome proliferator-activated receptor alpha in response to free fatty acids and is essential for skeletal muscle interleukin-6 production and signaling in diet-induced obesity. *J Biol Chem*. 2013;288:22193-22206.
 38. Walter DH, Rochwalsky U, Reinhold J, et al. Sphingosine-1-phosphate stimulates the functional capacity of progenitor cells by activation of the CXCR4-dependent signaling pathway via the S1P3 receptor. *Arterioscler Thromb Vasc Biol*. 2007;27:275-282.
 39. Cisneros BT, Law JJ, Matson ML, Azhdarinia A, Sevick-Muraca EM, Wilson IJ. Stable confinement of positron emission tomography and magnetic resonance agents within carbon nanotubes for bimodal imaging [published online ahead of print March 17, 2014]. *Nanomedicine (Lond)*. doi:10.2217/nnm.14.26.
 40. Bartneck M, Peters FM, Warzecha KT, et al. Liposomal encapsulation of dexamethasone modulates cytotoxicity, inflammatory cytokine response, and migratory properties of primary human macrophages [published online ahead of print March 7, 2014]. *Nanomedicine*. doi:10.1016/j.nano.2014.02.011.